2023 COASTAL MASTER PLAN

SCENARIO DEVELOPMENT: SEA LEVEL RISE AND ADDITIONAL CLIMATE-DRIVEN VARIABLES

ATTACHMENT B2

REPORT: VERSION 01

DATE: SEPTEMBER 2023

PREPARED BY: JAMES W. PAHL, ANGELINA M. FREEMAN, CATHERINE FITZPATRICK, KRISTA L. JANKOWSKI, & ERIC D. WHITE

COASTAL PROTECTION AND RESTORATION AUTHORITY
150 TERRACE AVENUE
BATON ROUGE, LA 70802
WWW.COASTAL.LA.GOV

COASTAL PROTECTION AND RESTORATION AUTHORITY

This document was developed in support of the 2023 Coastal Master Plan being prepared by the Coastal Protection and Restoration Authority (CPRA). CPRA was established by the Louisiana Legislature in response to Hurricanes Katrina and Rita through Act 8 of the First Extraordinary Session of 2005. Act 8 of the First Extraordinary Session of 2005 expanded the membership, duties, and responsibilities of CPRA and charged the new authority to develop and implement a comprehensive coastal protection plan, consisting of a master plan (revised every six years) and annual plans. CPRA's mandate is to develop, implement, and enforce a comprehensive coastal protection and restoration master plan.

CITATION

Pahl, J. W., Freeman, A. M, Fitzpatrick, C., Jankowski, K. L., & White, E. D. (2023). 2023 Coastal Master Plan: Attachment B2: Scenario Development: Sea Level Rise and Additional Climate-Driven Variables. Version I. (p. 43). Baton Rouge, Louisiana: Coastal Protection and Restoration Authority.

ACKNOWLEDGEMENTS

This document was developed as part of a broader Model Improvement Plan in support of the 2023 Coastal Master Plan under the guidance of the Modeling Decision Team:

- Coastal Protection and Restoration Authority (CPRA) of Louisiana – Stuart Brown, Ashley Cobb, Catherine Fitzpatrick (formerly CPRA), Krista L. Jankowski, David Lindquist, Sam Martin, and Eric White
- University of New Orleans – Denise Reed

This effort was funded by the Coastal Protection and Restoration Authority (CPRA) of Louisiana under Cooperative Endeavor Agreement Number 2503-12-58, Task Order No. 03.

EXECUTIVE SUMMARY

The Coastal Master Plan uses a scenario approach to aid in decision-making under uncertain future environmental conditions. Environmental drivers for the 2023 Coastal Master Plan scenario analysis include temperature and precipitation, two important drivers of change in coastal Louisiana.

Based on a review of climate literature it was determined that climate-related drivers such as temperature and precipitation will co-vary with the concentration of greenhouse gases in the atmosphere. The 2023 Coastal Master Plan scenario approach leverages Representative Concentration Pathways for greenhouse gas concentrations, Coupled Model Intercomparison Project data, and historical data to define scenario ranges for climate-related environmental drivers, including temperature and precipitation.

TABLE OF CONTENTS

LIST OF TABLES

LIST OF FIGURES

LIST OF ABBREVIATIONS

AR5 ..... FIFTH ASSESSMENT REPORT
ASOS ..... AUTOMATED AIRPORT WEATHER OBSERVATIONS
CMIP ..... COUPLED MODEL INTERCOMPARISON PROJECT
CPRA ..... COASTAL PROTECTION AND RESTORATION AUTHORITY
ERDC ..... ENGINEERING RESEARCH AND DEVELOPMENT CENTER
ET ..... EVAPOTRANSPIRATION
GMSL ..... GLOBAL MEAN SEA LEVEL
GRSL RISE ..... GULF-REGIONAL SEA LEVEL RISE
ICM ..... INTEGRATED COMPARTMENT MODEL
IPCC ..... INTERGOVERNMENTAL PANEL ON CLIMATE CHANGE
MSL ..... MEAN SEA LEVEL
NOAA ..... NATIONAL OCEANIC AND ATMOSPHERIC ADMINISTRATION
PET ..... POTENTIAL EVAPOTRANSPIRATION
RCP ..... REPRESENTATIVE CONCENTRATION PATHWAY
RSLR ..... RELATIVE SEA LEVEL RISE
SLR ..... SEA LEVEL RISE
SSP ..... SHARED SOCIOECONOMIC PATHWAY
TSS ..... TOTAL SUSPENDED SOLIDS
USACE ..... U.S. ARMY CORPS OF ENGINEERS
USGS ..... UNITED STATES GEOLOGICAL SURVEY

1.0 BACKGROUND

The Coastal Master Plan developed by the Louisiana Coastal Protection and Restoration Authority (CPRA) uses a scenario approach to aid in decision-making under uncertain future environmental conditions. Environmental drivers for the 2023 Coastal Master Plan scenario analysis were determined based on a review of the drivers used in the 2017 Coastal Master Plan, and include temperature and precipitation, two important drivers of change in coastal Louisiana (Appendix B: Scenario Development and Future Conditions).

Based on a review of climate literature (Melillo et al., 2014; Pachauri et al., 2014; Reidmiller et al., 2018; Sweet et al., 2017), it was determined that climate-related drivers such as temperature and precipitation will co-vary with the concentration of greenhouse gases in the atmosphere. Given uncertainties in how much greenhouse gas will be emitted into the atmosphere in the future, representative concentration pathways (RCPs) for greenhouse gas concentrations were developed by the Intergovernmental Panel on Climate Change (IPCC) for a plausible range of future concentrations. The RCPs are consistent with a range of possible future conditions, and the 2023 Coastal Master Plan scenario approach leverages the RCPs to define scenario ranges for climate-related environmental drivers. This attachment describes the process by which scenario values for temperature and precipitation were developed for the 2023 Coastal Master Plan, and how these ranges were then used to develop model boundary conditions for precipitation, evapotranspiration, air temperature, water temperature, and coastal tributary flowrates.

It was recognized early in the plan development process that independent climate modeling for the development of environmental scenarios around cohesive suites of variable values for use in the 2023 Coastal Master Plan would be cost, time, and computationally prohibitive. Instead, outputs from phase five of the Coupled Model Intercomparison Project (CMIP5) were leveraged for this planning process. Established by the World Climate Research Program, CMIP is an experimental protocol for studying the output of coupled atmosphere-ocean general circulation models that provides a community-based infrastructure in support of climate model diagnosis, validation, intercomparison, documentation, and data access. CMIP has been widely adopted by the international climate modeling community since its inception in 1995.

At the time of scenario development for the 2023 Coastal Master Plan in 2020, CMIP5 outputs that informed efforts such as the fifth assessment report of the IPCC (AR5) were the best available climate change projection data. Because of this, CMIP5 outputs were leveraged to provide climate-related variable projections for environmental scenarios. Since that time, the sixth assessment report (AR6) has been released and data from the sixth phase of CMIP6 is beginning to be made available. Data from the sixth phase of CMIP6 and other more recent studies will be considered in the development of environmental scenarios for future master plans.

2.0 SEA LEVEL RISE

Sea level rise (SLR) is one of the predominant environmental drivers of coastal habitat change and emergent wetland land loss in coastal Louisiana, both as a real phenomenon and within the broad set of habitat-change and project-effects models developed to inform CPRA's management decision-making. The preferred approach to accounting for SLR in a model development or update activity is to start by outlining the state of the science regarding sea level science, so that the development of specific SLR scenarios has a sound technical basis. The state of science on SLR is also complicated by the fact that it is a constantly-moving target, as new empirical data is collected and new global climate change models are developed. Importantly, however, over time the justification of particular SLR scenarios inevitably changes, which can result in confusion in, or criticism by stakeholders and the public about the changing narrative around SLR and other climate-driven factors. This adds to the importance of a sound state of the science declaration, and the incorporation of our best accounting for changing science, in that declaration.

2.1 UNCERTAINTIES FROM THE DEVELOPMENT OF THE 2017 COASTAL MASTER PLAN PLAUSIBLE RANGE AND SCENARIOS

The development of the 2017 Coastal Master Plan plausible range of values for future SLR (Pahl, 2017) was based on a review of the state of the science conducted in mid-to-late 2014. The development of the 2017 plausible range was based on earlier methodologies intent on ultimately defining smooth, constant linear or quadratic scenarios of future SLR. Framing minimum and maximum plausible scenarios allowed for the definition of an envelope of values between the two that was the "plausible range" from within which scenario values for use in numerical modeling were chosen.

Pahl (2017) chose to focus the 2017 plausible range and scenario development on Gulf-specific data, based on both empirical historical observations and projections of future Gulf-regional SLR (GRSL rise) that were different from global (eustatic) SLR. The emphasis of consideration of Gulf-regional data was carried through to the plausible range and scenario development process for the 2023 Coastal Master Plan.

For purposes of comparing 2017 to 2023 scenario development, deriving the minimum and maximum future scenarios for 2017 began with estimating the historical rate of GRSL rise based on empirical data from six tide gages along the presumed geologically-stable Gulf of Mexico coast (e.g., USACE 2009, 2011) and 1993-2014 satellite altimetry data, both developed by the National Oceanic and Atmospheric Administration (NOAA). Those two data sources averaged of 2.7 mm/yr GRSL rise. While the historical linear rate was needed for the U.S. Army Corps of Engineers (USACE) (2009, 2011) methodologies for developing the smoothed quadratic curves of future sea levels, that rate was also carried forward to establish the minimum (linear) scenario of the plausible range.

To develop the non-linear maximum of the plausible range for 2017, Coupled Model Intercomparison Project 3 and 5 outputs were considered. Although the CMIP5 outputs were considered more comprehensive than those from the older CMIP3, in 2014 the CMIP5 outputs were very recent. Both CMIP3 and CMIP5 output data were adjusted across the range of global scenarios for the Gulf based on observations in the historical record and in process-based modeling reported in Church et al. (2013).

The plausible range of GRSL rise outcomes for 2017 ranged from 0.31-1.98 m by the year 2100 from a year 2000 base. Pahl (2017) gave equal consideration to outputs from both process-based models and semi-empirical models, as both were still being considered by broader community. As well, Pahl (2017) considered the IPCC's four principal RCPs broadly considered by the field at the time (RCPs 2.6-8.5) equally likely. Therefore, neither model-type nor any particular RCP was weighted as "more likely" or "more definitive" in informing either the plausible range of values or the choice of scenarios.

Once the plausible range of 2000-2100 GRSL rise outcomes were developed, the quadratic definition of GRSL rise curves outlined in USACE (2009, 2011) was used to develop the curve of the plausible range maximum, and thus, when considered with the minimum based on the historical linear rate, define the plausible envelope of GRSL rise from within which specific scenarios would be chosen to apply to the 2017 project effects modeling.

Scenarios were chosen by the master plan modeling team, informed by modeler feedback that differences in year 2100 outcomes of 0.5 m were necessary to lead to differences in Integrated Compartment Model (ICM) outputs, and thus provide informative scenario-difference discussions. Tollefson (2020), reporting on interviews with the originators of the IPCC RCPs, highlighted the RCPs informing the CMIP5 modeling likewise were chosen to ensure that there would be differences in model outputs. With the 0.5 m difference in year 2100 criteria in hand, the master plan modeling team chose three scenarios from within the plausible 0.31 to 1.98 m GRSL rise envelope for application to the 2017 ICM-based project effects modeling: 1.0 m (Low Scenario), 1.5 m (Medium Scenario), and 1.98 m (High Scenario) GRSL rise by 2100 from a 2000 base year.

2.2 CONSIDERATION OF RECENT INFORMATION

One of the most important aspects of newer literature (2014-early 2021) from the standpoint of defining plausible future SLR curves for numerical modeling was the movement away from a smooth, continuous quadratic-based curve of values outlined for development in USACE (2009, 2011). Instead, the drafts of the analytical work outlined in the Working Group 1 report of the IPCC AR6 clearly illustrated assumptions of non-linear scenarios for projected future temperature and SLR increases (Figure 1). This change in projections required a corresponding change in approach of GRSL rise scenario development by CPRA for the 2023 Coastal Master Plan to one more directly reliant to the CMIP5 modeling data.

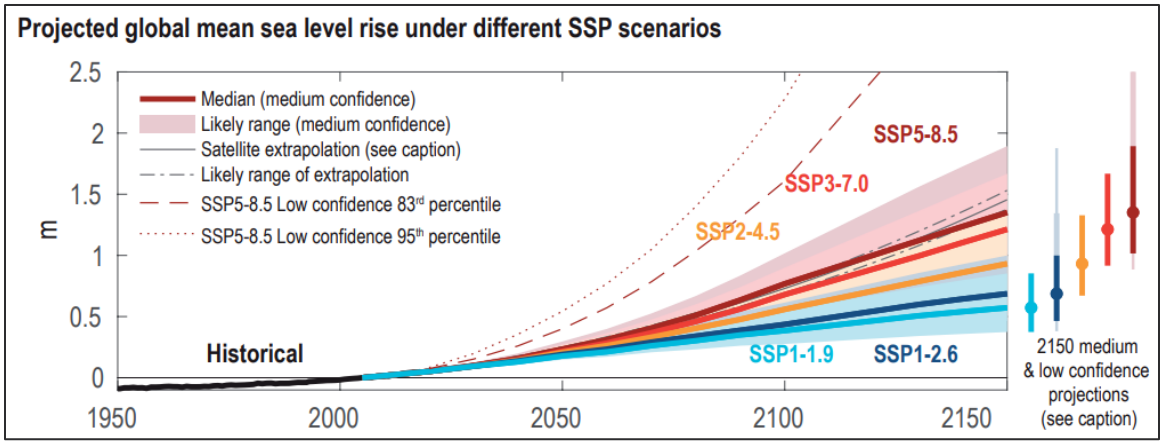

Figure 1. Projected global mean SLR from the Working Group 1 Report of the IPCC Sixth Assessment Report (Fox-Kemper et al., 2021).

2.3 PRIMARY SEA LEVEL RISE DATA SOURCE

Given the recognition that the USACE (2009/2011) approach to defining smooth, quadratic-based future SLR curves was no longer reflective of the CMIP modeling, the master plan modeling team decided to rely on the CMIP5 data itself to serve as the basis for the 2023 Coastal Master Plan SLR scenarios. Accordingly, staff downloaded Gulf-regional down-scaled and bias-corrected SLR data from the CMIP5 suite from http://gdo-dcp.ucllnl.org/downscaled_cmip_projections/. Ensemble data were downloaded for RCPs 2.6, 4.5, and 8.5.

2.4 CALCULATING GLOBAL MEAN SEA LEVEL PERCENTILE VALUES

To establish the GRSL rise datasets for the 2023 ICM model runs, the following *a priori* decisions were made by the modeling team:

- To mirror the data approach taken by the IPCC in its 2019 Special Report on the Ocean and Cryosphere in a Changing Climate, calculations for the SLR scenarios would use a calculated deviation (anomaly) from a 1986-2005 baseline average value instead of the raw data from the CMIP5 data files.
- Calibration/validation would use data up to 31 December 2019,
- Model spin-up with pre-defined boundary conditions would use 2019-2020 data, and
- 2023 model runs would use projected values for 1 January 2021 – 31 December 2070.

The master plan modeling team also decided that an *a priori* goal for analyzing and processing the CMIP model output SLR data was to calculate GRSL rise 5th-95th percentile distribution values to

match those defined by the IPCC (2019), plus an additional 99th percentile calculation. These calculations ultimately provided for a total of 18 plausible future GRSL rise curves: six percentiles (Table 1) for each of three RCPs (see below) to help frame the GRSL rise plausible range.

Each of the three RCP-specific files, "gmsl_26", "gmsl_45", and "gmsl_85" (for RCPs 2.6, 4.5, and 8.5, respectively), contained pre-calculated 5th, 50th, and 95th percentile values for 2007-2100. Each raw data file was originally read in Notepad but imported into Microsoft Excel to allow for data processing and visualization.

Table 1. Nomenclature associated with predictive model data percentiles. The 5th – 95th percentile Class nomenclatures match those of IPCC (2019).

Percentile	Class
5%	IPCC Low IPCC plausible
17%	IPCC Low likely
50%	IPCC Median
83%	IPCC High likely
95%	IPCC High plausible
99%	Additional

The left-hand and right-hand standard deviations for each RCP global mean sea level (GMSL) were calculated from the original data by subtracting the 5th percentile GMSL value from the 50th percentile GMSL value, or the 50th percentile GMSL value from the 95th percentile GMSL value, respectively. This value was then divided by 1.645, the Z-score for a normally-distributed (presumed) data distribution for the 5th and 95th percentiles (Figure 2).

$$Left\ \ SD = (50th\ \ Percentile\ \ Value - 5th\ \ Percentile\ \ Value)/1.645$$

And

$$Right\ \ SD = (95th\ \ Percentile\ \ Value - 50th\ \ Percentile\ \ Value)/1.645$$

where: 1.645 is the Z-score for the 5th/95th percentile.

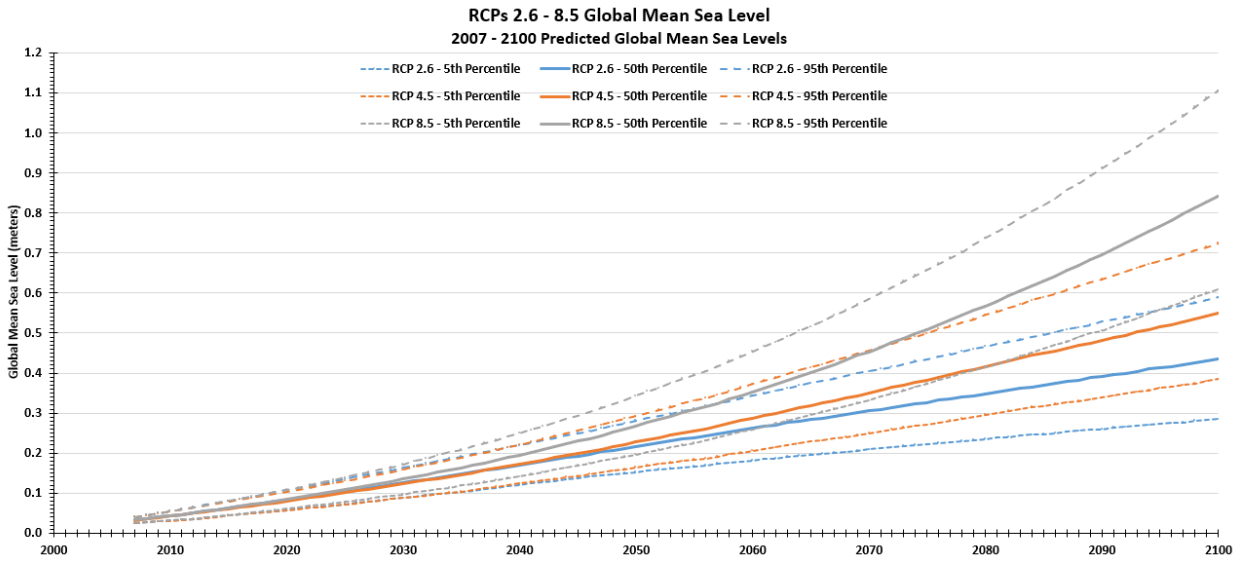

Figure 2. Mean annual global mean sea levels for 2007-2100 for RCPs 2.6, 4.5 and 8.5 from the CMIP5 ensemble model output dataset.

The 17th percentile GMSL value was estimated by multiplying the left-hand standard deviation by the 17th percentile Z-score of -0.954, and adding the product to the 50th percentile GMSL value. The 83rd and 99th percentile GMSL values were estimated by multiplying the right-hand standard deviation by the 83rd and 99th percentile Z-scores of 0.954 and 2.326, respectively, and adding that value to the 50th percentile GMSL value. These calculations led to estimated annual GMSL values for all six percentiles shown in Table 1, for all three RCPs discussed, from 2007 to 2100.

$$17th\ \ Percentile = 50th\ \ Percentile\ \ Value + (-0.954 * SD)$$

$$83rd\ \ Percentile = 50th\ \ Percentile\ \ Value + (0.954 * SD)$$

$$99th\ \ Percentile = 50th\ \ Percentile\ \ Value + (2.326 * SD)$$

2.5 ESTIMATING REGIONAL ADJUSTMENTS TO GLOBAL MEAN SEA LEVEL PERCENTILE VALUES

The full CMIP5 data download also contained a folder of .csv-formatted spreadsheets showing 20-year projected average regional mean sea levels (MSL) for individual latitude/longitude combinations on ½-degree increments for three specific periods in the future:

- 2040 (2030-2050),
- 2055 (2045-2065), and
- 2090 (2080-2100).

Within the median-value files for each RCP time increment file (e.g., “rsl_26-2040_median”), individual model projections of regional MSL from a rectangular area bounded by latitudes 28.9375°N to 30.9375°N and longitudes 89.0625°W to 94.0625°W (Figure 3) were averaged into a single value, giving nine unique values for each time period and *RCP combination.

The difference between the 2040, 2055, and 2090 regional MSL values and the corresponding GMSL values were calculated for each percentile. Presuming no difference at year 2000, difference values for the years 2000-2100 outside of 2000, 2040, 2055, and 2090 were estimated using interpolation. GMSL values were then adjusted to Louisiana coastal values relative to 2000 through subtraction of the annual differences from the original and estimated (see below) GMSL values. The average percent of original GMSL represented by each annual correction to Louisiana regional MSL increased from the 5th through the 95th percentile (Table 2). Percent deviation between GMSL and Louisiana-specific global relative sea level values decreased in most cases as RCP increased. Across all percentiles, average percent deviation was 27.7% for RCP 2.6, 23.6% for RCP 4.5, and 22.9% for RCP 8.5.

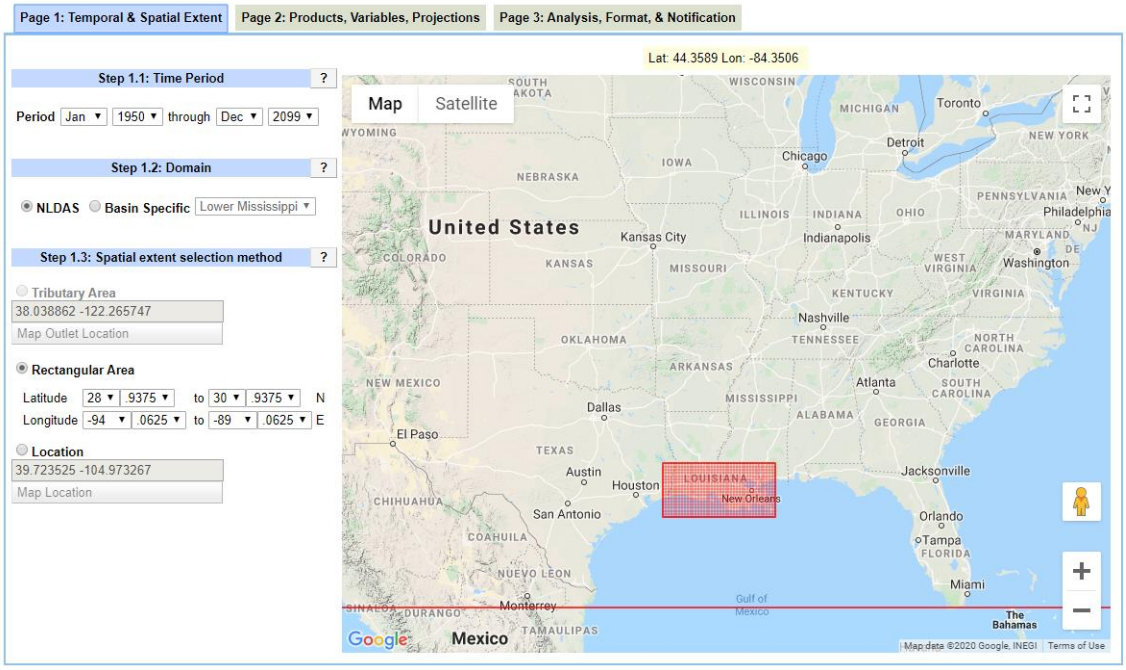

Figure 3. Spatial extent of the “Louisiana-regional” MSL data that were surveyed to inform the development of GRSL rise.

Table 2. Summary of Percent Deviation of Calculated Louisiana-specific Mean Sea levels from CMIP5-derived Global Mean Sea Levels

RCP	Percentile					
	5th	17th	50th	83rd	95th	99th
2.6	15.9 (10.1-19.9)	22.5 (15.3-25.6)	26.7 (18.4-32.1)	30.9 (21.6-38.4)	34.5 (23.7-44.0)	35.4 (24.1-45.5)
4.5	10.4 (6.3-11.6)	18.0 (10.6-22.4)	22.9 (13.4-29.5)	27.3 (16.2-35.6)	31.1 (18.6-40.9)	32.1 (19.2-42.3)
8.5	11.7 (2.4-15.0)	18.0 (6.6-22.4)	22.3 (9.4-31.6)	26.0 (12.1-37.3)	29.3 (14.3-42.3)	30.1 (14.9-43.7)

To facilitate visual examination of the 18 sea level curves, all Louisiana-adjusted MSL values were plotted as a time series, from 2000 to 2100. For comparative purposes, Louisiana-regional SLR data for the six scenarios presented in Sweet et al. (2017) were overlaid on the regionalized CMIP5 data.

2.6 DEVELOPMENT OF THE PLAUSIBLE RANGE OF GULF-REGIONAL SEA LEVEL RISE SCENARIOS

We can define one version of a plausible range of Louisiana-specific GRSL rise from the breadth of GRSL rise estimated from the CMIP5 RCPs and the Sweet et al. (2017) data (Figure 4). As seen in Figure 4, several of the Sweet et al. (2017) scenarios were substantially higher than the envelope of values calculated from the CMIP5 scenarios data download; particularly the Sweet et al. regional intermediate-high, regional high, and regional extreme scenarios. Ignoring the Sweet et al. (2017) regionally adjusted extreme scenario (it was not carried into the Sweet et al. (2022) scenario considerations, which although not used to inform the 2023 scenarios is used here to help establish context), the plausible range of 2000-2100 GRSL rise between the Sweet et al. (2017) regionally adjusted low scenario curve and that of the Sweet et al. (2017) regionally adjusted high scenario is 0.34–2.5 m.

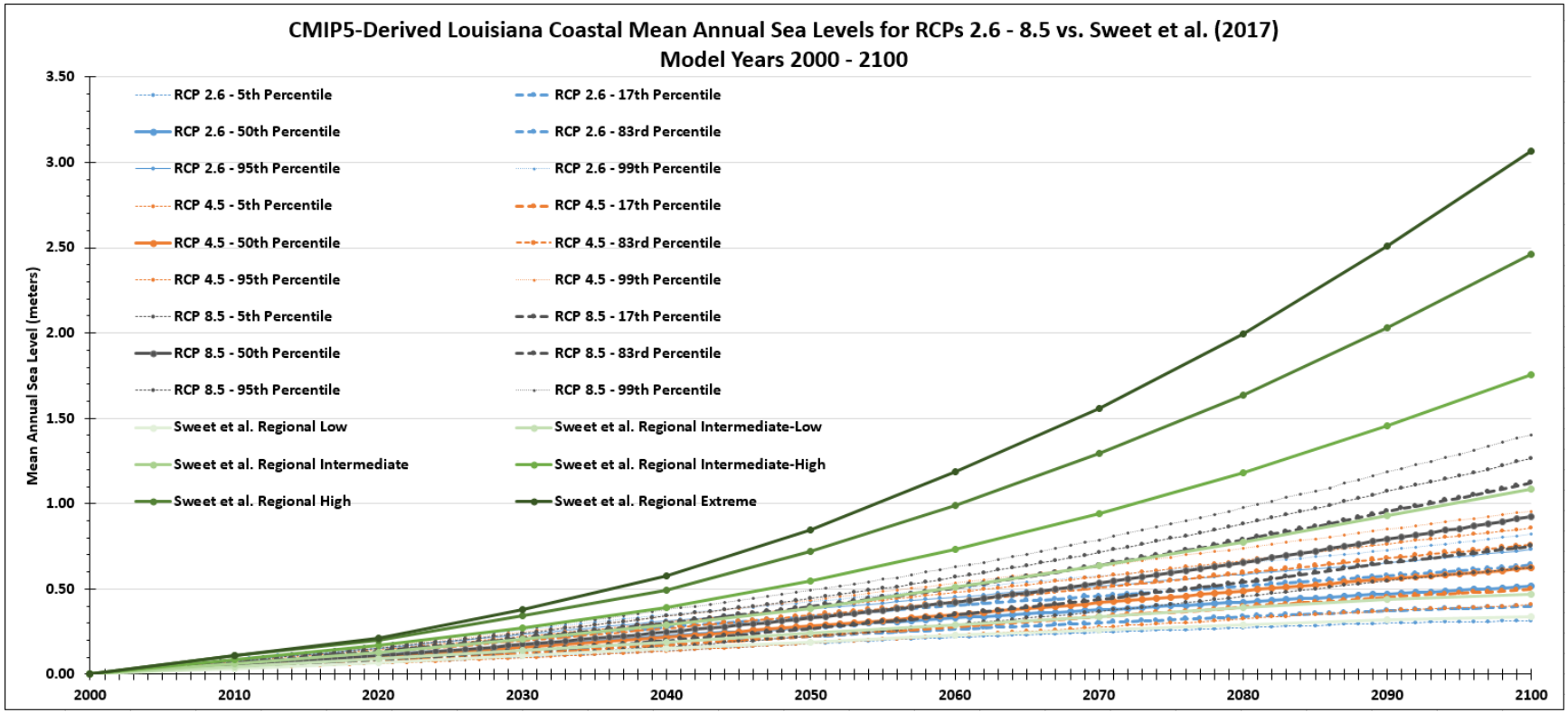

Figure 4. The full inventory of regionalized SLR curves defining the 2023 Coastal Master Plan plausible range and serving as candidate scenarios for numerical modeling.

2.7 SELECTION OF SCENARIOS FOR GULF-REGIONAL SEA LEVEL RISE FOR THE 2023 COASTAL MASTER PLAN

Similar to modeler input into the selection of GRSL rise scenarios for the 2017 plan, discussions with the ICM modeling team suggested the need to have 2100 GRSL rise scenarios differ in projected sea level by approximately 0.5–.20 m at the end of the 50-year period of analysis ending in 2070. With that criterion in place, the master plan modeling team chose the regionally adjusted NOAA Intermediate and regionally adjusted NOAA Intermediate High Scenarios as the two scenarios for use in the 2023 numerical modeling-based evaluations of candidate projects. The regionally adjusted NOAA Intermediate Scenario was nearly identical to the regionally adjusted RCP 8.5 – 83rd Percentile curve (Figure 4). Additional scenarios within the plausible range were used to explore finer sensitivities in the model suite and in project outcomes.

2.8 RECOGNIZED UNCERTAINTIES FROM DEFINING THE 2023 SEA LEVEL RISE SCENARIOS, AND RECOMMENDATIONS FOR THE 2029 COASTAL MASTER PLAN UPDATE

One of the critical uncertainties that remains from the 2023 plausible range and scenario development effort is the issue of environmental scenario likelihoods. Specifically, the likelihood that a particular RCP (or, in future, Shared Socioeconomic Pathways, or SSPs) will actually occur in the future remains highly uncertain. Greater clarity on underlying scenario likelihood might allow for a weighting of the scenario-specific GRSL rise curves and could influence the decision on scenario adoption. Although there was a definition of scenario likelihood in Sweet et al. (2017, 2022), a careful reading of the information in both of those reports illustrates that they were referencing the likelihood of a particular RCP or SSP leading to a specific sea level, which is not the same as the likelihood of the RCP itself occurring.

The analysis and results outlined in this report will be subject to reconsideration by CPRA in the years leading up to the conduct of the numerical modeling in support of the 2029 master plan update. The recommendation is that CPRA undertake a similar analytical approach in the future as was taken here, using the most up-to-date and available CMIP model ensemble results. Those models, likewise subject to constant updating to account for the state of the science, represent the most up-to-date expression of mechanistic understanding of the impact of greenhouse gases and global warming scenarios on sea level components.

The suite of model outputs considered should be limited only to those models that appear to model the Gulf of Mexico to an appropriate level. That point was mentioned in the discussions in a Sea Level Rise Workshop that was held in Baton Rouge in April 2022, concurrent with the 2022 Gulf of Mexico Conference. Exclusion of specific, poorer-performing models within the CMIP ensemble from the data

considerations of Louisiana- or Gulf-regional SLR will influence the values for each RCP/SSP*percentile scenario. CPRA hopes that between the writing of this report and the expected date that the 2029 SLR scenario needs to be defined, likely in 2026 or early 2027, that the Gulf research and management community can provide some clarity to this need and any model evaluation criteria.

2.9 SUPERIMPOSITION OF SEA LEVEL RISE ON TIDAL BOUNDARY

Once GRSL rise curves were identified for each future scenario, the long-term trend needed to be superimposed onto an hourly tidal boundary at the Gulf of Mexico boundary in the ICM-Hydro model. ICM-Hydro utilizes an hourly time series representing astronomic tidal waters, to which the long-term GRSL rise trend was added. In addition to the astronomic tidal component, ICM-Hydro incorporates several other tidal water level constituents that occur at varied timescales. First, a seasonal variation on Gulf waters is applied due to summer/winter temperature impacts on water levels. Second, elevated water levels due to storm surge from tropical storms and hurricanes are applied for the 5-10 day window in which the synthetic storms are assumed to occur in the ICM simulations (Attachment B4). Finally, a subtidal residual is applied that captures water level fluctuations that are the result of wind events, frontal passages, and other short-term (e.g., days-to-week) deviations from a purely astronomic tidal signal.

To build this hourly non-GRSL rise tidal boundary condition, observed water levels from six tide stations located within the ICM model domain were analyzed and decomposed to the constituent tidal components. Further analysis was done on the tidal decomposition to remove relative SLR signatures from the observed tidal records by fitting a linear trend to the long-term, uncorrected tidal water levels. The slope of this trend line was then compared against the long-term mean eustatic SLR in the Gulf of Mexico (Gulf) as monitored by NOAA's Laboratory for Satellite Altimetry[1]. The difference between the site-specific relative SLR and the Gulf-mean was then taken to be the site-specific subsidence rate. The Gulf-mean sea level trend and the site-specific subsidence rate were then also removed from the tidal signal. This resulted in an observed hourly water level time series that could be used as a boundary condition in the model where each of the tidal constituents could be added back in, after being adjusted for modeled storms (storm surge component, see Attachment B4), subsidence (scenario-specific value, see Attachment B3), or GRSL rise (see above). For all scenarios, data for the 2010 calendar year was used to build both the decomposed astronomic tidal signal and the subtidal residual (representing winds/fronts). Observed, gridded wind data for the calendar year 2010 was used, so that every model year had wind and wave calculations within ICM-Hydro that corresponded to the same time period that was used to build the subtidal boundary condition.

[1] https://www.star.nesdis.noaa.gov/socd/lsa/SeaLevelRise/LSA_SLR_timeseries_regional.php

3.0 CO-VARYING TEMPERATURE AND PRECIPITATION SCENARIOS WITH SEA LEVEL RISE

3.1 SUMMARY OF SEA LEVEL RISE SCENARIO DEVELOPMENT

Sea level rise is one of the most important environmental drivers of coastal change and wetland loss in coastal Louisiana, and one of the most impactful on the 2017 Coastal Master Plan ICM's projections of landscape change (Meselhe et al., 2017). Therefore, SLR curves were the first environmental scenario variables selected. They were selected based on a literature review, and regionally adjusting global climate model data. For SLR scenario development, the initial suite of curves included the three curves for the 2017 Coastal Master Plan (Meselhe et al., 2017), six additional curves developed by NOAA (Sweet et al., 2017), and CMIP5 derived curves for RCPs 2.6, 4.5, and 8.5. For the 2023 Coastal Master Plan scenario analysis, a SLR curve for the lower scenario corresponds with the plausible range associated with RCP 4.5. The SLR curve for the higher scenario corresponds with the plausible range associated with RCP 8.5.

3.2 CO-VARYING ENVIRONMENTAL BOUNDARY CONDITIONS WITH SEA LEVEL RISE SCENARIOS

Once the SLR curves were selected and an associated RCP was identified, it was necessary to obtain co-varying projections of precipitation and temperature to include in the two environmental scenarios for project selection. As was done for sea level projections, CMIP5 precipitation and temperature data for ensembles of model runs was downloaded for the coastal Louisiana region. The data, as described in the following sections, was analyzed so that the most appropriate (e.g., least biased) CMIP5 dataset could be used to develop projections of future environmental conditions that correspond to the selected SLR scenarios being used for simulations.

As discussed in further detail, the CMIP5 temperature data corresponding to the median RCP 4.5 and RCP 8.5 outputs was used to develop future scenario boundary conditions of air temperature, riverine water temperature, estuarine water temperature, and evapotranspiration for the 2023 Coastal Master Plan simulations. Precipitation data from these same CMIP5 datasets was used to develop future scenario boundary conditions for daily precipitation and daily flowrates for all rivers tributary to the Louisiana coastal rivers. Trends from the CMIP5 precipitation projections within the coastal zone were used directly to develop flowrates for all non-Mississippi River tributaries (described below). Due to the decoupled nature of the Mississippi River flow hydrograph from coastal zone precipitation trends, a separate methodology was used for the Mississippi River. CMIP5 precipitation projections for the

entire Mississippi River Basin were used to run a continental scale hydrologic mode; ensemble hydrographs for the Mississippi River at Tarbert Landing (e.g., immediately downstream of the Old River Control Structure) were used to develop the Mississippi River boundary condition.

4.0 TEMPERATURE-DERIVED BOUNDARY CONDITIONS

4.1 HISTORIC MEAN TEMPERATURES AND PROJECTED TEMPERATURE ANOMALIES FROM CMIP5 DATA

Historic temperature data from 1985 to 2019 were downloaded (on February 11, 2020) for coastal Louisiana stations from the Louisiana automated weather observations (ASOS) monitoring network from the Iowa Mesonet archive[2] (Table 3).

Table 3. Historic temperature data coastal Louisiana station names and locations

Station Code	Station Name	LAT	LON
7R3	Amelia/Lake Palourde	29.69306	-91.0986
7R4	Intracoastal City	29.78	-92.13
7R5	Cameron Heliport	29.7833	-93.3
9F2	Fourchon(SAWRS)	29.1	-90.2
ARA	New Iberia/Acadiana	30.03776	-91.8839
BTR	Baton Rouge Ryan Airport	30.53722	-91.1469
BVE	Boothville	29.33333	89.4075
HUM	Houma	29.5665	-90.6604
LCH	Lake Charles Municipal Airport	30.12472	-93.2283
LFT	Lafayette Airport	30.2115	-91.981
MSY	New Orleans Airport	29.9933	-90.2511
NEW	New Orleans Lakefront	30.04239	-90.0283
S58	South Timbalier	28.53333	-90.5833

Baseline average monthly temperatures from 1986 to 2005 were computed from the ASOS dataset. Average temperatures were computed across all stations. Average monthly temperatures ranged from a low of 12.1˚ C in January, to a high of 28.0˚C in July (Figure 5 and Table 4).

[2] https://mesonet.agron.iastate.edu/request/download.phtml?network=LA_ASOS

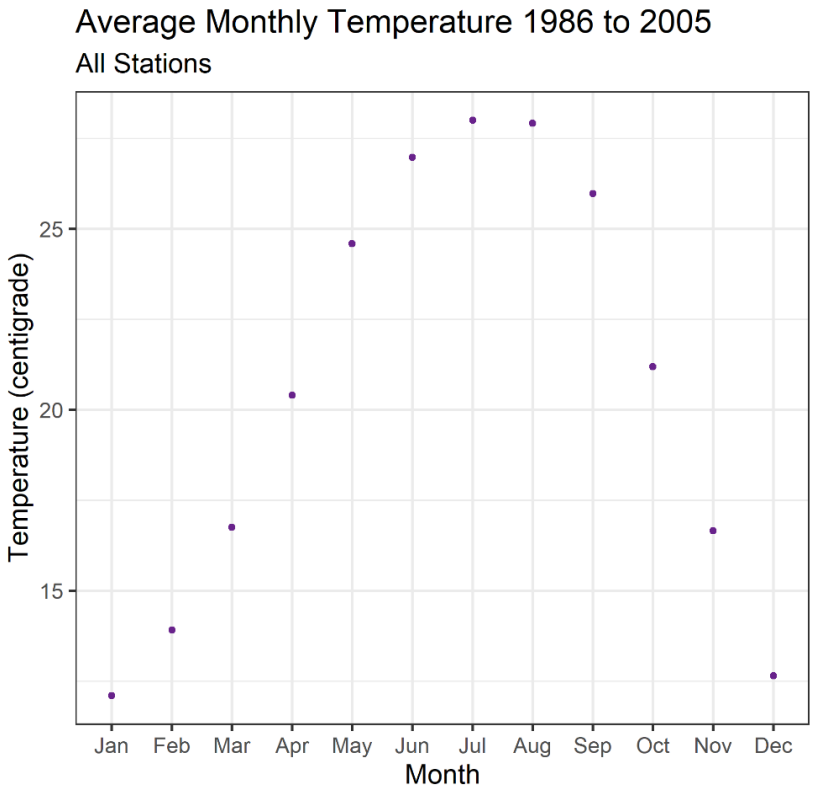

Figure 5. Average monthly temperatures for all coastal Louisiana ASOS stations from 1986 to 2005.

Table 4. Summary of 1986-2005 average temperature benchmarks from historical data

Month	Temperature (˚C)	Month	Temperature (˚C)
January	12.1	July	28.0
February	13.9	August	27.9
March	16.8	September	26.0
April	20.4	October	21.2
May	24.6	November	16.7
June	27.0	December	12.7

The monthly baseline temperature values were used to develop temperature anomaly projections for different RCPs. This was done by subtracting the long-term baseline averages from the 2019-2099 CMIP5 model forecasts. The resulting temperature anomaly time series were then used to set boundary conditions for ICM simulations, as described below.

4.2 DAILY MEAN AIR TEMPERATURE

For each RCP analyzed, a temperature anomaly time series was generated by subtracting monthly projections for the years 2019 through 2070 from the long-term mean calculated from ASOS stations. The resulting time series of CMIP5-projected monthly temperature anomalies were temporally downscaled to daily temperature anomalies using the spline interpolation function in MATLAB[3]. This daily temperature anomaly time series was then converted to daily mean temperature by adding the anomaly to the long-term daily mean air temperature for the coastal zone. This procedure is shown, schematically in Figure 6.

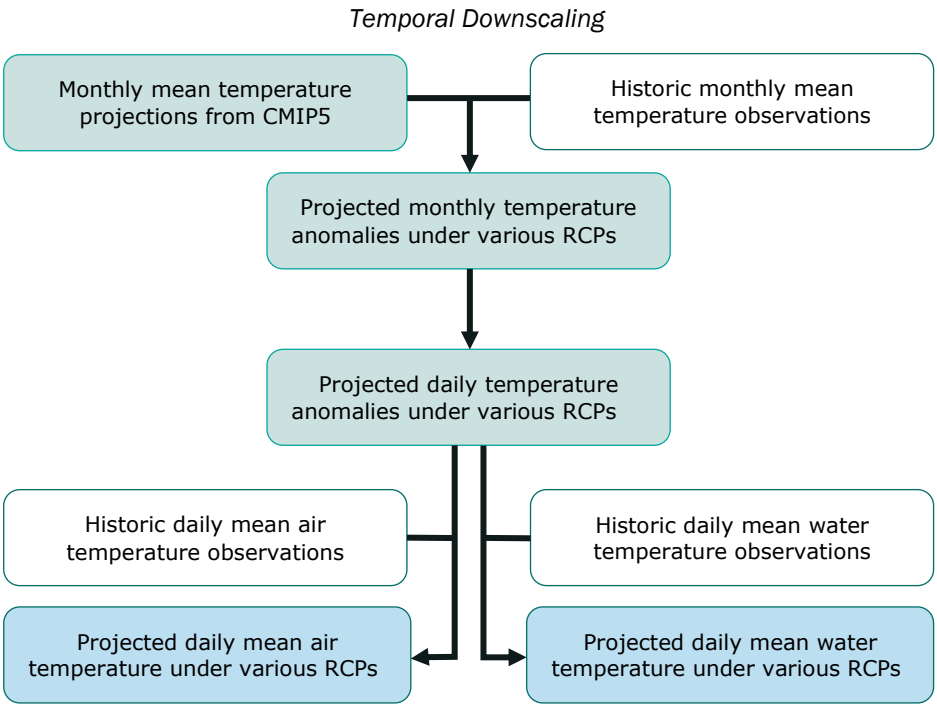

Figure 6. Process used to develop daily temperature projections (blue) from observed records (white) and CMIP5 projections (green).

The long-term daily time series used to determine mean daily temperature was from 1981-2010 for the Baton Rouge area, as provided by the National Weather Service[4]. Note that since the completion of this analysis, the long-term daily average temperatures provided by the National Weather Service have been updated to represent the 1991-2020 period. Future master plan analyses will update

[3] https://www.mathworks.com/help/matlab/ref/interp1.html

[4] https://www.weather.gov/wrh/Climate?wfo=lix

these long-term means as necessary.

The constructed daily air temperature time series for the lower project selection scenario (S07) which corresponded to RCP 4.5 is shown in Figure 7. Data for additional scenarios is provided in Supplemental Material B2.1.

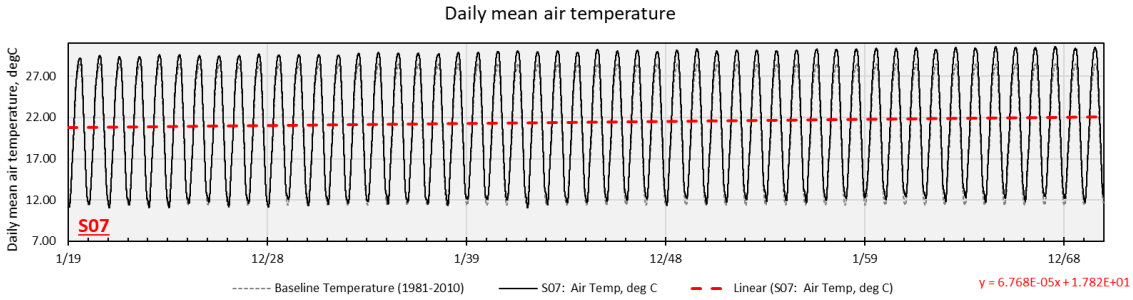

Figure 7. Daily mean air temperature for the lower project selection scenario (S07). This corresponds to RCP 4.5. Note the long-term trend increase of 6.768x10-5 °C/day. This corresponds to an average temperature increase of 1.29 °C over the 52-year simulation period, which starts in 2019.

4.3 DAILY MEAN WATER TEMPERATURE

Two long-term monitoring stations operated by the United States Geological Survey (USGS) were used to develop water temperature boundary conditions. The first was for the Mississippi River water temperature, which shows a stronger seasonal variation than coastal water due to the prevalence of snowmelt and runoff from colder regions in the northern U.S. (this difference can be seen in Figure 8 and Figure 9). For local/coastal waters, a temperature record for Barataria Bay was used.

For the two water temperature stations, the entire available record was used to develop baseline mean daily temperature time series. For Mississippi River water temperature, the observed record from 2004 through 2020 at the Baton Rouge gage[5] was used to calculate daily mean river water temperatures (Figure 8). For estuarine and coastal waters, the observed record from 2001 through 2020 at the Barataria Bay near Grand Terre gage[6] was used to calculated daily mean estuarine water

[5] https://waterdata.usgs.gov/nwis/dvstat?referred_module=sw&site_no=07374000&por_07374000_61163=197857,00010,61163,2004-10-01,2019-11-05&format=html_table&stat_cds=mean_va&date_format=YYYY-MM-DD&rdb_compression=file&submitted_form=parameter_selection_list

[6] https://waterdata.usgs.gov/nwis/dvstat?referred_module=sw&site_no=291929089562600&por_291929089562600_61811=1973707,00010

temperature (Figure 9).

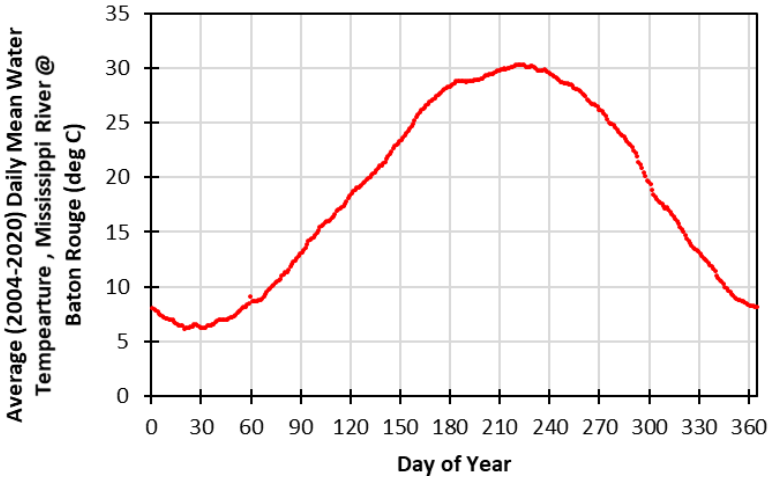

Figure 8. Daily mean water temperature from 2004-2020 for the Mississippi River at Baton Rouge (USGS NWIS site 07374000).

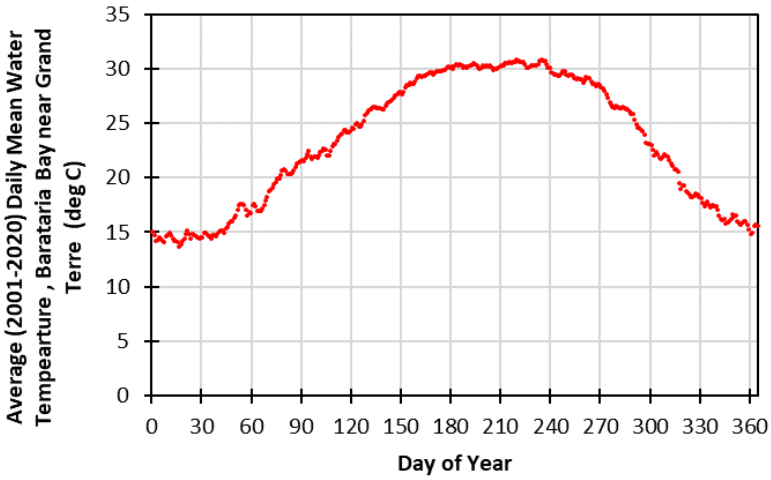

Figure 9. Daily mean water temperature from 2004-2020 for the Mississippi River at Baton Rouge (USGS NWIS site 291929089562600).

These observed daily mean water temperatures were adjusted for future climate projections by adding the mean values to the projected daily air temperature anomalies calculated via the method described

,61811,2001-12-05,2020-08-10&format=html_table&stat_cds=mean_va&date_format=YYYY-MM-DD&rdb_compression=file&submitted_form=parameter_selection_list

above.

The constructed daily water temperature time series for the lower project selection scenario (S07) which corresponded to RCP 4.5 is shown in Figure 10, for river temperature, and in Figure 11 for estuarine temperature. Data for additional scenarios is provided in Supplemental Material B2.1.

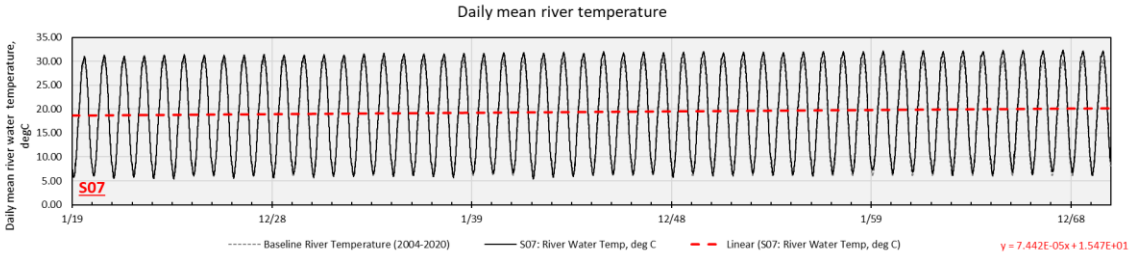

Figure 10. Daily mean river water temperature for the lower project selection scenario (S07).

Figure 10 corresponds to RCP 4.5. Note the long-term trend increase of 6.768×10^{-5} °C/day. This corresponds to an average water temperature increase of 1.29 °C over the 52-year simulation period, which starts in 2019. This is the same magnitude of increase as seen in the air temperature change over time.

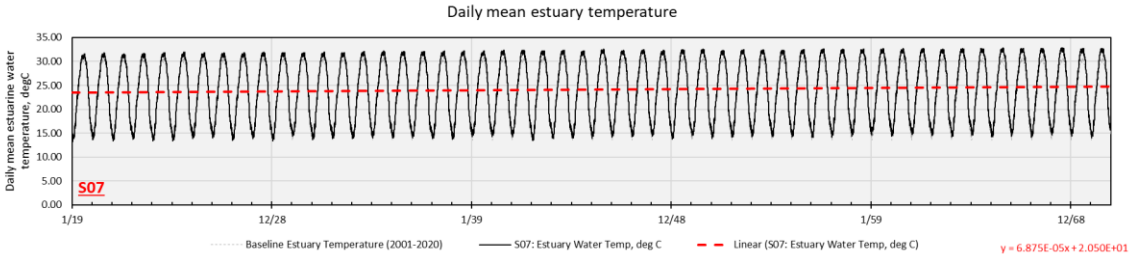

Figure 11. Daily mean estuarine water temperature for the lower project selection scenario (S07).

Figure 11 corresponds to RCP 4.5. Note the long-term trend increase of 6.768×10^{-5} °C/day. This corresponds to an average water temperature increase of 1.29 °C over the 52-year simulation period, which starts in 2019. This is the same magnitude of increase as seen in the air temperature change over time.

4.4 DAILY MEAN POTENTIAL EVAPOTRANSPIRATION

In addition to developing daily time series of air and water temperatures, the CMIP5 temperature anomalies were also used to calculate a daily time series of potential evapotranspiration (PET) for ICM

simulations. There are many methods available to calculate potential evapotranspiration, which can be "broadly classified as *radiation*, *temperature*, *combination*, or *evaporation-pan* methods" (Chin, 2006). Given the direct calculation of temperature anomalies from CMIP5 datasets used above, a temperature-based method was used to calculate PET; the Hargreaves-Samani (1982, 1985) method was selected given the relative simplicity to incorporate temperature projections into the calculations. Necessary solar radiation constants required by Hargreaves-Samani (1985) for a latitude of 30° N were calculated following methodologies published by the United Nations Food and Agriculture Organization (Allen et al., 1998).

The constructed daily PET time series for the lower project selection scenario (S07) which corresponded to RCP 4.5 is shown in Figure 12. The data for additional scenarios, as well as the full set of calculations for the Hargreaves-Samani (1985) method are provided in Supplemental Material B2.1.

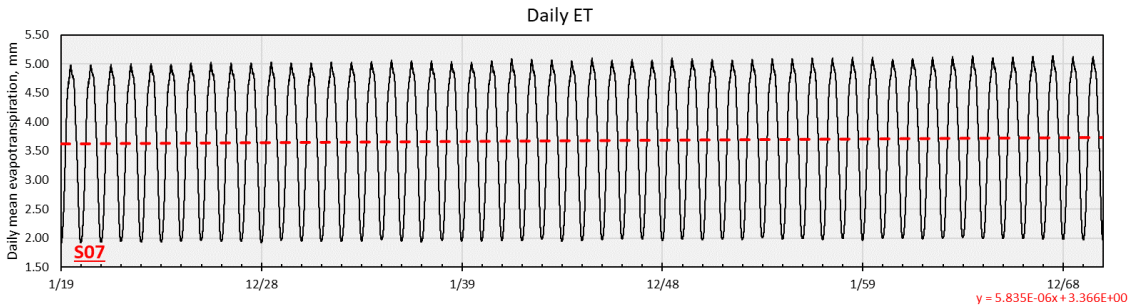

Figure 12. Daily mean potential evapotranspiration raters for the lower project selection scenario (S07)

Figure 12 corresponds to RCP 4.5. Note the long-term trend increase of 5.835×10^{-6} mm-H_2O/day. This corresponds to an average PET rate increase of 0.11 mm-H_2O/day at the end of 52-year simulation period, which starts in 2019.

5.0 PRECIPITATION-DERIVED BOUNDARY CONDITIONS

5.1 CMIP5 HINDCAST COMPARISON TO OBSERVED

Precipitation data for RCPs 2.6, 4.5, and 8.5 were downscaled and corrected for bias. Precipitation values were calculated from the hindcast of the 1986-2006 baseline period from the downloaded CMIP5 data files.

Precipitation units were in mm/day, and therefore were converted to monthly mm values by multiplying by the number of days in each month. Precipitation data are contained in both climate and hydrology CMIP5 model datasets (Figure 13 and Figure 14). A comparison of precipitation baseline results from CIMP5 climate and hydrology datasets, and historical data from the NOAA Atlas New Orleans airport station and Lake Charles https://www.weather.gov/wrh/climate?wfo=lch station illustrate the similarity among data trends (Figure 15). The CMIP5 climate precipitation data was selected for use in the 2023 Coastal Master Plan scenario values.

Historical data were obtained from the National Weather Service, and used to analyze whether historical observations fall within the range of values from the CMIP5 climate model data on both monthly (Figure 16) and seasonal (Figure 17) bases.

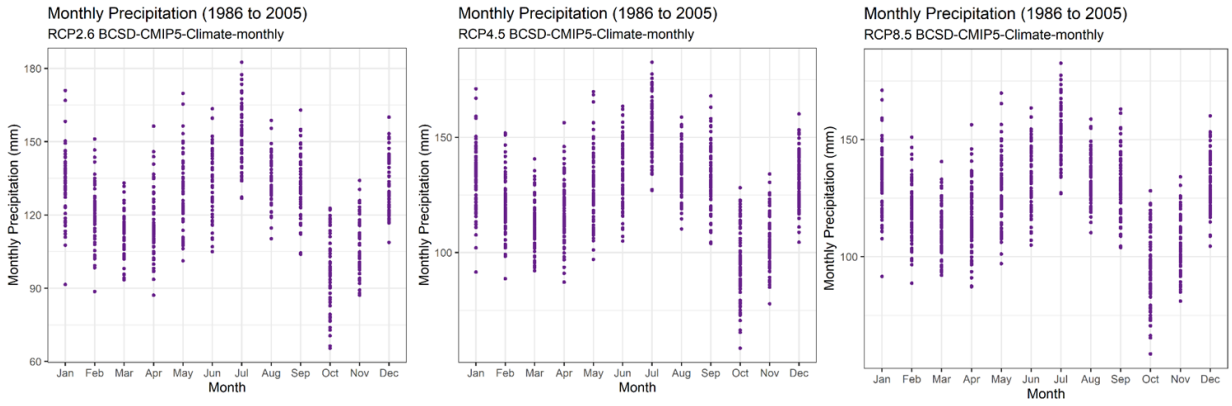

Figure 13. Mean monthly precipitation values from CMIP5 climate dataset, 1986 to 2005.

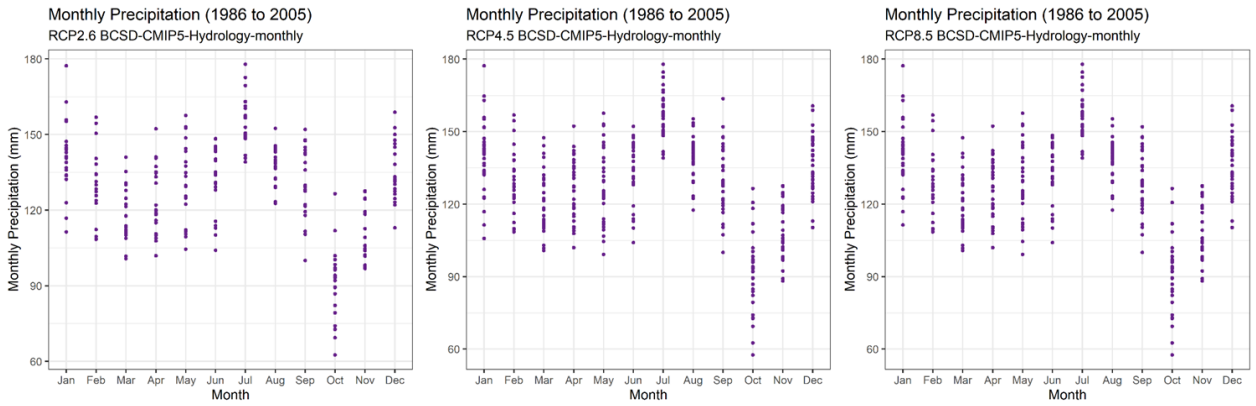

Figure 14. Mean monthly precipitation values from CMIP5 hydrology dataset, 1986 to 2005.

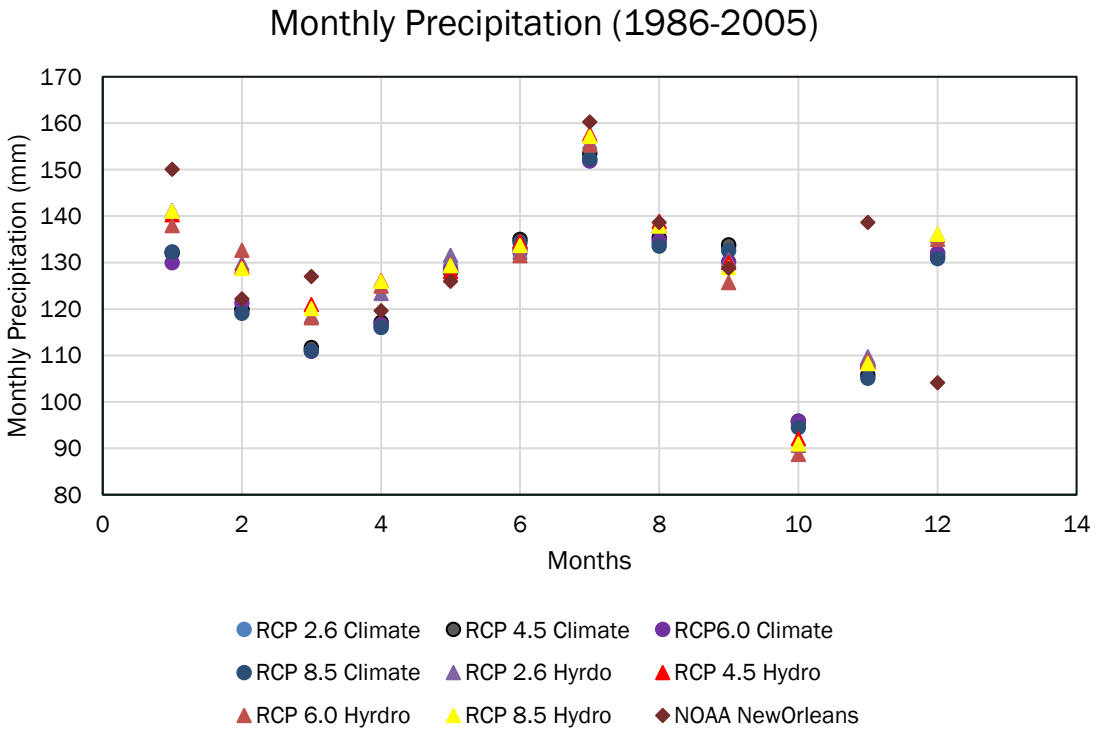

Figure 15. Comparison of monthly precipitation data from CMIP5 climate and hydro datasets, and historical precipitation data.

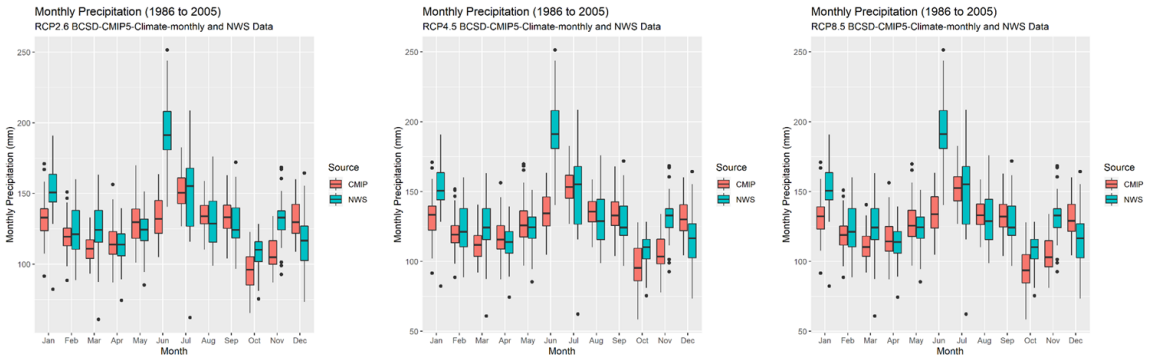

Figure 16. Mean monthly precipitation CMIP5 climate data and historical National Weather Service data, 1986 to 2005.

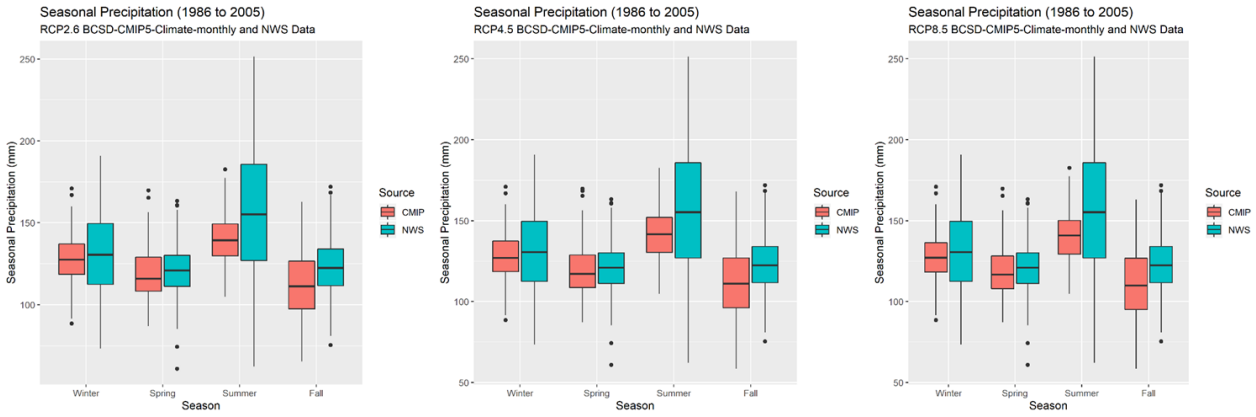

Figure 17. Mean seasonal precipitation CMIP5 climate data and historical National Weather Service data.

To further compare the precipitation model data to historical data, monthly (Table 5) and seasonal (Table 6) bias between the two datasets was computed using the equation:

$$PBias = \frac{O - P}{O} * 100\%$$

Where: P = mean of the predicted values

O = mean of observed values.

Table 5. Precipitation metrics for CMIP5 climate data and historical National Weather Service data, monthly bias and percent bias from 1986 to 2005

	RCP 2.6		RCP 4.5		RCP 8.5	
Month	**Bias (mm)**	**Bias (%)**	**Bias (mm)**	**Bias (%)**	**Bias (mm)**	**Bias (%)**
Jan	21.19	0.14	21.05	0.14	20.95	0.14
Feb	3.73	0.03	3.65	0.03	4.55	0.04
Mar	15.10	0.12	14.77	0.12	15.46	0.12
Apr	-2.73	-0.02	-3.83	-0.03	-2.74	-0.02
May	-6.10	-0.05	-5.04	-0.04	-4.98	-0.04
Jun	60.09	0.31	58.21	0.30	58.86	0.30
Jul	-1.24	-0.01	-2.70	-0.02	-1.62	-0.01
Aug	-3.32	-0.03	-4.52	-0.03	-2.73	-0.02
Sep	-5.07	-0.04	-5.39	-0.04	-4.16	-0.03
Oct	13.12	0.12	12.78	0.12	14.13	0.13
Nov	23.96	0.18	25.78	0.20	26.52	0.20
Dec	-14.60	-0.12	-13.90	-0.12	-13.46	-0.11

Table 6. Precipitation bias metrics for CMIP5 climate data and historical National Weather Service data, seasonal bias and percent bias from 1986 to 2005

	RCP 2.6		RCP 4.5		RCP 8.5	
Season	**Bias (mm)**	**Bias (%)**	**Bias (mm)**	**Bias (%)**	**Bias (mm)**	**Bias (%)**
Fall	10.67	0.09	11.06	0.09	12.16	0.10
Spring	2.09	0.02	1.97	0.02	2.58	0.02
Summer	18.51	0.12	17.00	0.11	18.17	0.11
Winter	3.44	0.03	3.60	0.03	4.01	0.03

5.2 SEASONAL WETNESS

Precipitation data from CMIP5 was accessed in monthly averages, however the models require daily precipitation and tributary flowrates. Temporally downscaled precipitation data from CMIP5 can have unrealistically large values of precipitation for any individual day; therefore to avoid numerical instabilities and other spurious impacts no temporal downscaling of precipitation data was performed. Rather, CMIP5 projections of monthly precipitation values were used to develop a time series of *seasonal wetness*. Initially five wetness classes were analyzed: very dry, dry, average, wet, and very

wet.

Using model output available from the CMIP5 analysis, precipitation data was analyzed for a variety of projected IPCC environmental scenarios (RCP 4.5 & RCP 8.5) for the 21st century. For the time frame from 2019 through 2070 (the 2023 Coastal Master Plan future simulation period), the output precipitation time series was extracted and normalized by the long-term mean precipitation from observed records to develop a precipitation anomaly time series from 2019 through 2070.

For the 52-year precipitation anomaly time series, each season (winter, spring, summer, fall) was classified as being: drier than average, wetter than average, or of average wetness.

The classification of wetness was defined as *average wetness* if the mean volume during any given season was within ±0.3 standard deviations of the long-term seasonal mean volume (Figure 18). Any season above this threshold was defined as *wet*, and any season with less volume was defined as *dry*. This approach was originally developed by analyzing the log-transformed flowrates for all tributaries to the coastal zone; if the observed records perfectly followed a log-normal distribution using a threshold of 0.3 standard deviations results in 23.6% of all seasons being classified as *average wetness*, 38.2% classified as *wet*, and 38.2% classified as *dry* (Rice, 2007).

While this approach was developed from hydrograph analysis of observed records, the same ±0.3 standard deviations threshold was applied to the CMIP5 future projections of rainfall to classify all future seasons as being drier, wetter, or average when compared to the long-term observed rainfall records in coastal Louisiana. The time series of calculated wetness classification for RCP 4.5 and RCP 8.5 precipitation projections for coastal Louisiana are shown in Figure 19 and Figure 20, respectively.

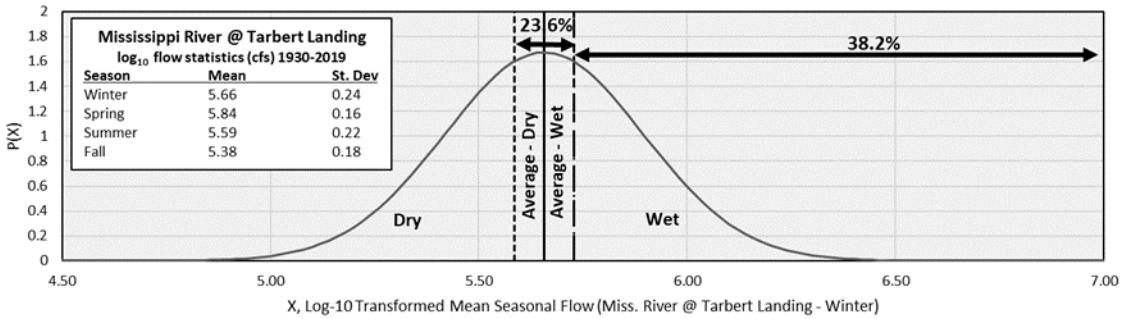

Figure 18. Log-normal distribution and wetness classifications for Mississippi River winter flow statistics at Tarbert Landing (1930-2019).

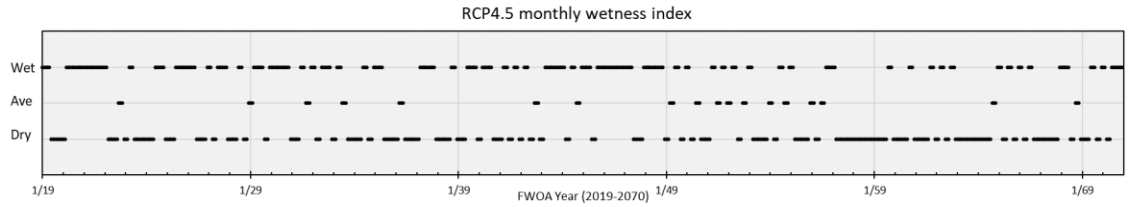

Figure 19. Wetness index, as derived from the RCP 4.5 CMIP5 precipitation anomalies.

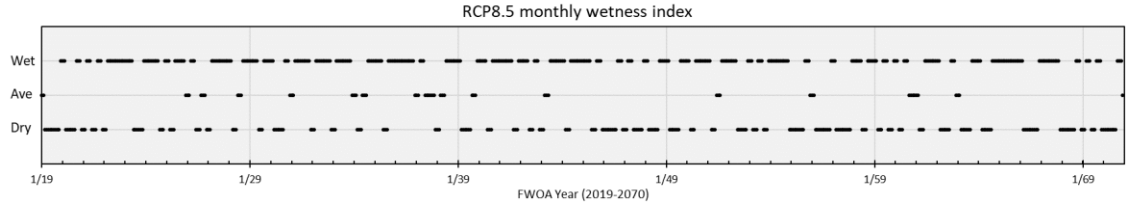

Figure 20. Wetness index, as derived from the RCP 8.5 CMIP5 precipitation anomalies.

5.3 COASTAL TRIBUTARY DAILY MEAN FLOWRATES

Once the future scenario 52-year time series of seasonal wetness were identified (Figure 19 and Figure 20), the historic record of coastal tributary flowrates was examined to identify, for each coastal zone tributary, a representative observed hydrograph that represents each seasonal wetness class. For example, in the Calcasieu River, the observed record for Spring 2012 was identified as being a historically dry spring; Spring 2013 was an average spring, and Spring 2017 was a historically wet spring. Therefore, in the future scenario, any year that was identified in the CMIP5 precipitation anomaly to be wetter than average, the Spring 2017 hydrograph was used as the representative flow in the Calcasieu River. The representative season for each tributary/wetness class combination as well as the classification of all seasons in the full observed record for each tributary is provided in Supplemental Material B2.2. The last 14 days of a given season were used to linearly interpolate between the two seasonal hydrographs to avoid any sudden discontinuities in the daily flow boundary conditions.

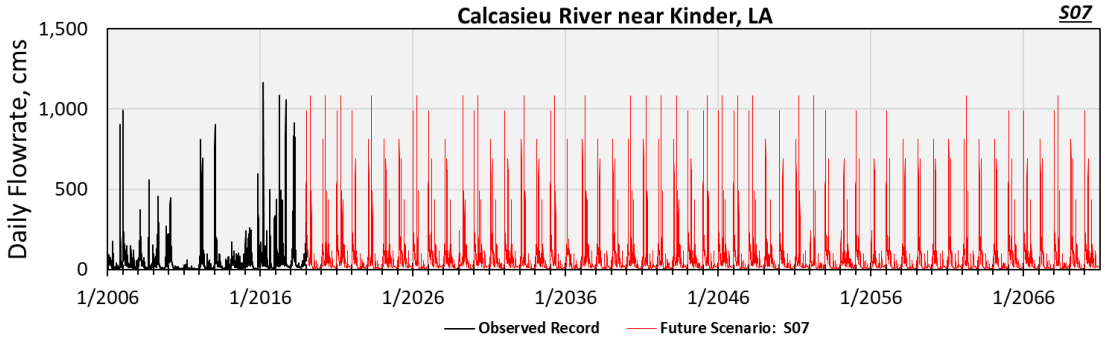

Figure 21. Daily flow hydrograph of the Calcasieu River for hindcast period (black, 2006-2018) and the lower project selection future scenario (S07).

Figure 21 correlates to a wetness index derived from RCP 4.5 precipitation projections (red, 2019-2070). Data for additional scenarios and/or coastal tributaries are provided in Supplemental Material B2.2.

Prior to selecting representative seasons from the historic record, the daily flow time series of all coastal tributaries were collected from USGS river gages. Following the methodology developed for the 2017 Coastal Master Plan (Brown, 2017), missing flow data, as well as un-gaged basins, were filled using rating curves from nearby stations. The rating curves and all processed tributary data are included in Supplemental Material B2.2.

5.4 MISSISSIPPI RIVER DAILY MEAN FLOWRATES

It should be noted that all of the seasonal wetness analysis discussed above applies to all coastal zone tributaries except the Mississippi and Atchafalaya Rivers. For those, since they are dependent upon continental-scale processes (as opposed to coastal zone precipitation), model output for the Mississippi River at Tarbert Landing was provided by USACE Engineering Research and Development Center (ERDC). Researchers at ERDC modeled, using continental-scale rainfall-runoff models, daily hydrographs for 16 simulations (all derived from CMIP5 rainfall time series under RCP 4.5) for the Mississippi River at Tarbert Landing. An ensemble average of these 16 simulations was used to set the daily flowrate in the Mississippi River at Tarbert Landing, as well as the Atchafalaya River (assuming that the Tarbert Landing equaled 70% of the total Mississippi River flow, and 30% was diverted through the Old River Control Structure into the Atchafalaya system).

Rather than using the true ensemble mean of these 16 runs, the ensemble mean +0.6 standard deviations was selected. This value was used since using the true ensemble mean would dramatically underpredict the springtime flood peak in all 52 years. Adjusting the ensemble mean upward by 0.6 standard deviations managed to match the mean springtime flood peak while keeping the additional freshwater during low-flow periods to a minimum. Please refer to Supplemental Material B2.3 for the

methodology and a discussion of the continental scale hydrologic modeling conducted by ERDC; and refer to Supplemental Material B2.4 for additional analysis and discussion concerning developing the ensemble mean hydrograph for the Mississippi River at Tarbert Landing.

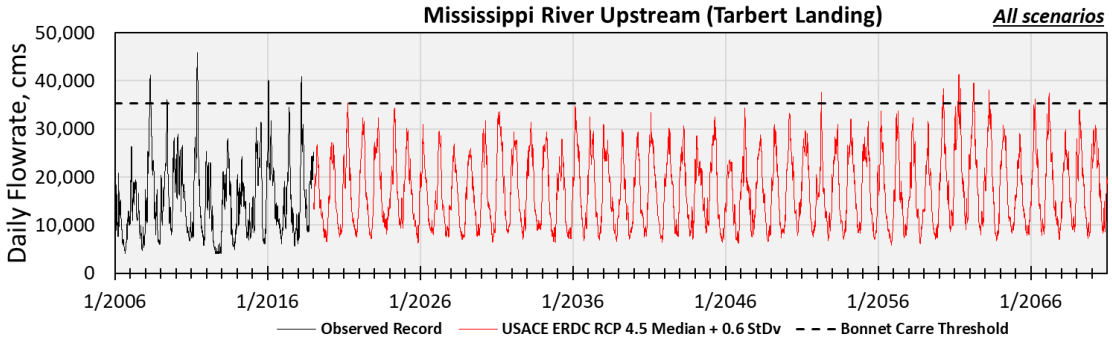

Figure 22. Daily flow hydrograph of the Mississippi River at Tarbert Landing hindcast period (black, 2006-2018) and the lower project selection future scenario (S07). This is derived from RCP 4.5 precipitation projections (red, 2019-2070). Note the dashed horizontal line which denotes the operational threshold for opening the Bonnet Carre Spillway.

5.5 SUSPENDED SEDIMENT CONCENTRATIONS

Once tributary flowrate time series were generated, a sediment rating curve was applied to each respective tributary to develop the future scenario suspended sand and fines sediment concentration time series. The Mississippi River and the Atchafalaya River both had sediment particle size analyses completed on the observational data available from USGS, so these two rivers had separate sand and fines flow-dependent rating curves developed. The Mississippi River suspended sediment concentrations utilize a rating curve which took hysteresis into account for seasonal flood impacts on suspended sediment concentrations in the Mississippi River (Meselhe et al., 2016; Allison et al., 2012). All other coastal tributaries, however, had limited sediment particle size data available and therefore utilized a flow-dependent rating curve for total suspended solids (TSS). The calculated TSS concentration was then partitioned into suspended sand and suspended fines using the following assumptions.

First, the daily total suspended sediment (silts and clays with D50 < 0.625 mm; sands with D50 > 0.625 mm) was calculated from the daily flowrate and sediment-discharge rating curves. Next a flow-dependent *sand fraction* was calculated by comparing the suspended sand concentration to the suspended fines concentration seen in the Mississippi River suspended sediment data across all observed flowrates (Figure 23). This resulted in a relationship in which sand suspension begins at approximately 35% of peak discharge, and exponentially increases such that approximately 75% of all sand in suspension will occur at 60% of peak discharge. This method assumes that the maximum

sand in suspension occurs at the peak discharge in the river.

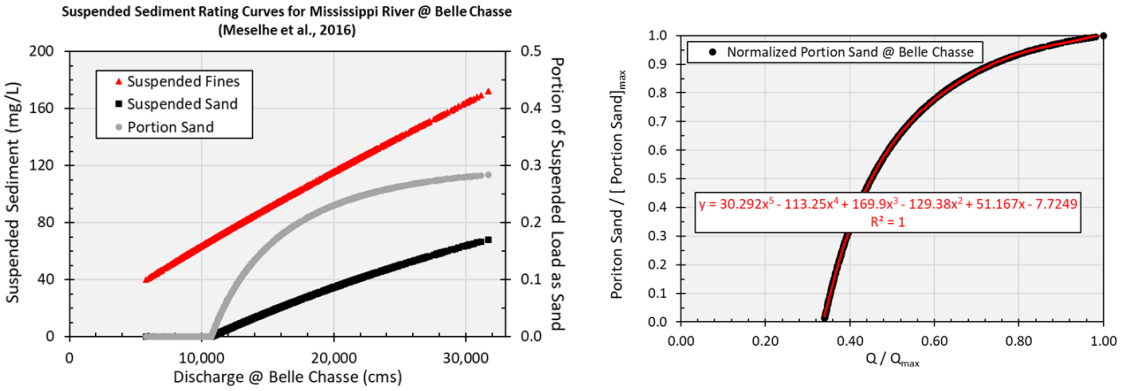

Figure 23. Sand-to-fines ratio as a function of Mississippi River flow (left), and a generic flow-dependent sand fraction of TSS (right).

This flow-dependent sand fraction curve was then compared to the flow-dependent sand fraction in the Mississippi River at Belle Chasse (Figure 24, gray dots), which indicated that the sand fraction reaches a maximum of 29% of suspended sediment concentrations in the Mississippi River. This sand-fraction curve was then used to partition calculated TSS concentrations into sand and fines for all non-Mississippi and non-Atchafalaya Rivers in the coastal zone. There was a dearth of data to quantitatively inform these sand fractions for most rivers, so the modeling team assumed that all rivers east of the Mississippi River, which are predominantly sandy rivers, would have a maximum sand fraction of 30% (Figure 24, red dots), roughly equivalent to the relationship of the Mississippi River. Coastal tributaries west of the Mississippi River were assumed to have much less sand present, and a maximum sand fraction of 10% was assumed for all of these western tributaries (Figure 24, black dots).

As previously mentioned, the above method used to develop separate time series for suspended sand and suspended fines required calculated concentrations of TSS. When enough paired discharge-TSS data was available from USGS, a gage-specific TSS rating curve was used for each respective tributary. However, most of the tributaries in the coastal zone did *not* have enough paired data to develop TSS rating curves. When this was the case, two different methods were used to develop a TSS rating curve. For rivers east of the Mississippi River (e.g., the Florida Parishes) rating curves for TSS were developed by Roblin (2008) from drainage area, discharge, and turbidity observations. For rivers west of the Mississippi River (excluding the Atchafalaya), data from all tributaries were combined into a single, larger, dataset to develop an estimated rating curve. Given the sparse data available for these rivers, a sediment load rating curve was developed; which then needed to be reverted to a concentration for use as a model boundary condition. All sediment rating curves and analyses are provided in Supplemental Materials B2.5 and Supplemental Materials B2.6.

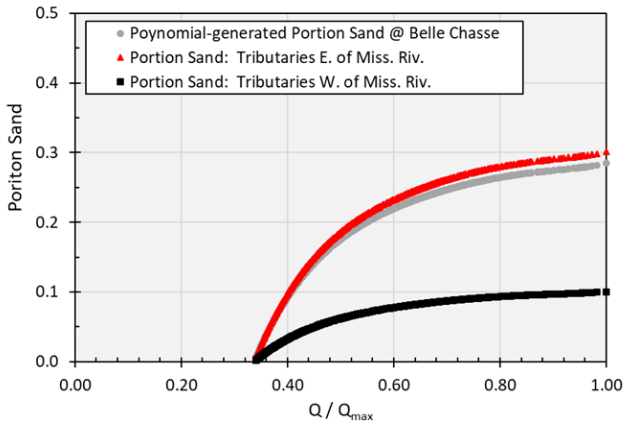

Figure 24. Flow-dependent sand fraction of TSS for the Mississippi River at Belle Chasse (gray) and assumed sand fractions for tributaries. Tributaries located east of the Mississippi River (red) were assumed to have a maximum sand fraction of 30%, and assumed sand fractions for tributaries west of the Mississippi River (excluding Atchafalaya River) (black) which were assumed to have a maximum sand fraction of 10%.

5.6 DAILY PRECIPITATION

As discussed above, CMIP5 precipitation data was analyzed for a variety of projected IPCC RCPs for the 21st century. For the time frame from 2019 through 2070 (the 2023 Coastal Master Plan future simulation period), the output precipitation time series was extracted and normalized by the long-term mean precipitation from observed records to develop a precipitation anomaly time series from 2019 through 2070. Following the same methodology as for tributary flows, the 52-year precipitation anomaly time series was converted to a seasonal wetness.

Following an approach similar to the representative hydrographs used for tributary flow, representative seasons were identified from the observed rainfall data in coastal Louisiana for the period 2006 through 2018. The rainfall data for each representative wet/average/dry season was then used for the corresponding seasonal wetness index time series for RCP 4.5 and RCP 8.5 (Figure 19 and Figure 20). The observed rainfall data used to selective representative seasons from was a gridded rainfall dataset developed for the Louisiana coastal zone for the 2006 to 2018 time frame (Sharif, 2019). Unlike the tributary flow observational data where a unique representative season was selected for each individual tributary, a single representative season was used for the entire model domain of gridded rainfall. The representative season was chosen to be the same period that was selected as the representative seasonal hydrograph for the Tickfaw River. The Tickfaw was selected since it is a relatively small watershed without any large upstream reservoirs. Therefore, it was assumed to have a

hydrologic response that is relatively tightly coupled to rainfall within the coastal zone.

Once the daily precipitation time series was developed from representative seasons of gridded rainfall, the boundary conditions needed to be updated to account for rainfall from during tropical storms. For each of the synthetic storms imposed upon the ICM future scenario boundary conditions (Attachment B4) the synthetic gridded rainfall data was extracted to the same resolution as the existing gridded rainfall data. During the time period in which the storm was assumed to be present (generally a 5-10 day period, depending upon the synthetic storm characteristics) the storm rainfall superseded the representative seasonal rainfall in the daily future scenario boundary conditions.

The constructed daily precipitation time series for multiple future scenarios which corresponded to each RCP are provided in Supplemental Material B2.7.

6.0 REFERENCES

Allen, R. G., Pereira, L. S., Raes, D., & Smith, M. (1998). Chapter 3: Meteorological Data in Crop evapotranspiration - Guidelines for computing crop water requirements - FAO Irrigation and drainage paper 56. Food and Agriculture Organization of the United Nations. Rome, Italy

Allison, M. A., Demas, C. R., Ebersole, B. A., Kleiss, B. A., Little, C. D., Meselhe, E. A., Powell, N. J.,Pratt, T. C., Vosburg, B. A., 2012. A water and sediment budget for the lower Mississippi–Atchafalaya River in flood years 2008–2010: implications for sediment discharge to the oceans and coastal restoration in Louisiana. *Journal of Hydrology*. 432, 84–97.

Brown, S. (2017). *2017 Coastal Master Plan Modeling: Attachment C3-26: Hydrology and Water Quality Boundary Conditions*. Version Final. (pp. 1-44). Baton Rouge, Louisiana: Coastal Protection and Restoration Authority.

Chin, D. A. (2006). *Water Resources Engineering, 2nd Edition.* Pearson Prentice Hall. Upper Saddle River, NJ, USA.

Church, J. A., Clark, P. U., Cazenave, A., Gregory, J. M., Jevrejeva, S., Levermann, A., Merrifield, M. A., . . . Unnikrishnan, A. S. (2013). *Sea Level Change.* In T. F. Stocker, D. Qin, G.-K. Plattner, M. Tignor, S.K. Allen, J. Boschung, A. Nauels, Y. Xia, V. Bex and P.M. Midgley (Eds.), Climate Change 2013: The Physical Science Basis. Contribution of Working Group I to the Fifth Assessment Report of the Intergovernmental Panel on Climate Change. Cambridge, United Kingdom and New York, NY, USA: Cambridge University Press

Fox-Kemper, B., H.T. Hewitt, C. Xiao, G. Aðalgeirsdóttir, S.S. Drijfhout, T.L. Edwards, N.R. Golledge, M. Hemer, R.E. Kopp, G. Krinner, A. Mix, D. Notz, S. Nowicki, I.S. Nurhati, L. Ruiz, J.-B. Sallée, A.B.A. Slangen, and Y. Yu, (2021) *Ocean, Cryosphere and Sea Level Change.* In Climate Change 2021: The Physical Science Basis. Contribution of Working Group I to the Sixth Assessment Report of the Intergovernmental Panel on Climate Change [Masson-Delmotte, V., P. Zhai, A. Pirani, S.L. Connors, C. Péan, S. Berger, N. Caud, Y. Chen, L. Goldfarb, M.I. Gomis, M. Huang, K. Leitzell, E. Lonnoy, J.B.R. Matthews, T.K. Maycock, T. Waterfield, O. Yelekçi, R. Yu, and B. Zhou (eds.)]. Cambridge University Press, Cambridge, United Kingdom and New York, NY, USA, pp. 1211–1362, doi:10.1017/9781009157896.011.

Habib, E., Meselhe, E., & White, E. (2017). *Coastal Master Plan: Attachment C2–3: Precipitation and Evapotranspiratio*n. Version Final. Baton Rouge, Louisiana: Coastal Protection and Restoration Authority.

Hargreaves, G.H. and Z.A. Samani (1982). Estimating potential evapotranspiration. *Journal of Irrigation and Drainage Engineering*, ASCE. 108(3): 225-230.

Hargreaves, G.H. and Z.A. Samani (1985). Reference-crop evapotranspiration from temperature.

Applied Engineering in Agriculture. 1(2): 96-99.

IPCC (2019). IPCC Special Report on the Ocean and Cryosphere in a Changing Climate [H.-O. Pörtner, D.C. Roberts, V. Masson-Delmotte, P. Zhai, M. Tignor, E. Poloczanska, K. Mintenbeck, A. Alegría, M. Nicolai, A. Okem, J. Petzold, B. Rama, N.M. Weyer (eds.)]. Cambridge University Press, Cambridge, UK and New York, NY, USA, 755 pp. https://doi.org/10.1017/9781009157964.

Melillo, J. M., Richmond, T., & Yohe, G. (2014). *Climate change impacts in the United States. Third national climate assessment*, 52.

Meselhe, E., White, E. D., & Reed, D. J. (2017). *2017 Coastal Master Plan: Appendix C: Modeling Chapter 2 - Future Scenarios.* Version Final. Baton Rouge, Louisiana: Coastal Protection and Restoration Authority.

Meselhe, E.A., K.M. Sadid, & M.A. Allison. (2016). Riverside morphological response to pulsed sediment diversions. *Geomorphology*. 270, 184-202.

Pachauri, R.K., Allen, M.R., Barros, V.R., Broome, J., Cramer, W., Christ, R., Church, J. A., Clarke, L., Dahe, Q., & Dasgupta, P. (2014). *Climate change 2014: synthesis report. Contribution of Working Groups I, II and III to the fifth assessment report of the Intergovernmental Panel on Climate Change*. IPCC.

Pahl, J. (2017). 2017 *Coastal Master Plan: Attachment C-2: Eustatic Sea Level Rise*. Version Final. Baton Rouge, Louisiana: Coastal Protection and Restoration Authority. 23 pp. http://coastal.la.gov/wp-content/uploads/2017/04/Attachment-C2-1_FINAL_3.16.2017.pdf.

Reidmiller, D., Avery, C. W., Easterling, D. R., Kunkel, K. E., Lewis, K., Maycock, T. K., & Stewart, B. C. (2018). *Fourth national climate assessment. Volume II: Impacts, Risks, and Adaptation in the United States*, 440.

Rice, J.A. (2007). *Mathematical Statistics and Data Analysis, 3rd Edition*. Brooks/Cole Cengage India. Noida, Uttar Pradesh, India.

Roblin, Rachel J. 2008. *Water Quality Modeling of Freshwater Diversions in the Pontchartrain Estuary.* University of New Orleans Theses and Dissertations. 693. https://scholarworks.uno.edu/td/693/.

Sharif, R.B., Habib, E.H., ElSaadani M. (2019). Evaluation of Radar-Rainfall Products of Coastal Louisiana. *Remote Sensing.* 12(9) 1447.

Sweet, W.V., R.E. Kopp, C.P. Weaver, J. Obeysekera, R.M. Horton, E.R. Thieler, and C. Zervas (2017). Global and Regional Sea Level Rise Scenarios for the United States. NOAA Technical Report NOS CO-OPS 083. National Oceanic and Atmospheric Administration, National Ocean Service, Center for Operational Oceanographic Products and Services, Silver Spring, MD, 75 pp.

https://tidesandcurrents.noaa.gov/publications/techrpt83_Global_and_Regional_SLR_Scenarios_for_the_US_final.pdf.

Sweet, W.V., B.D. Hamlington, R.E. Kopp, C.P. Weaver, P.L. Barnard, D. Bekaert, W. Brooks, M. Craghan, G. Dusek, T. Frederikse, G. Garner, A.S. Genz, J.P. Krasting, E. Larour, D. Marcy, J.J. Marra, J. Obeysekera, M. Osler, M. Pendleton, D. Roman, L. Schmied, W. Veatch, K.D. White, and C. Zuzak (2022). Global and Regional Sea Level Rise Scenarios for the United States: Updated Mean Projections and Extreme Water Level Probabilities Along U.S. Coastlines. NOAA Technical Report NOS 01. National Oceanic and Atmospheric Administration, National Ocean Service, Silver Spring, MD, 111 pp. https://oceanservice.noaa.gov/hazards/sealevelrise/noaa-nos-techrpt01-global-regional-SLR-scenarios-US.pdf.

Tollefson, J. (2020). How hot will Earth get by 2100? Nature 580: 444-446.

United States Army Corps of Engineers. (2009). *Water resource policies and authorities incorporating sea-level change considerations in civil works programs*. Circular No. 1165-2-211.

United States Army Corps of Engineers. (2011). *Water resource policies and authorities incorporating sea-level change considerations in civil works programs.* Circular No. 1165-2-212.